

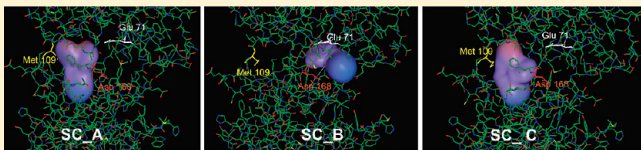
# Using Consensus-Shape Clustering To Identify Promiscuous Ligands and Protein Targets and To Choose the Right Query for Shape-Based Virtual Screening

Violeta I. Pérez-Nueno<sup>\*†</sup> and David W. Ritchie<sup>†</sup>

<sup>†</sup>INRIA Nancy, LORIA, 615 rue du Jardin Botanique, 54600 Villers-lès-Nancy, France

 Supporting Information

**ABSTRACT:** Ligand-based shape matching approaches have become established as important and popular virtual screening (VS) techniques. However, despite their relative success, many authors have discussed how best to choose the initial query compounds and which of their conformations should be used. Furthermore, it is increasingly the case that pharmaceutical companies have multiple ligands for a given target and these may bind in different ways to the same pocket. Conversely, a given ligand can sometimes bind to multiple targets, and this is clearly of great importance when considering drug side-effects. We recently introduced the notion of spherical harmonic-based “consensus shapes” to help deal with these questions. Here, we apply a consensus shape clustering approach to the 40 protein–ligand targets in the DUD data set using PARASURF/PARAFIT. Results from clustering show that in some cases the ligands for a given target are split into two subgroups which could suggest they bind to different subsites of the same target. In other cases, our clustering approach sometimes groups together ligands from different targets, and this suggests that those ligands could bind to the same targets. Hence spherical harmonic-based clustering can rapidly give cross-docking information while avoiding the expense of performing all-against-all docking calculations. We also report on the effect of the query conformation on the performance of shape-based screening of the DUD data set and the potential gain in screening performance by using consensus shapes calculated in different ways. We provide details of our analysis of shape-based screening using both PARASURF/PARAFIT and ROCS, and we compare the results obtained with shape-based and conventional docking approaches using MSSH/SHEF and GOLD. The utility of each type of query is analyzed using commonly reported statistics such as enrichment factors (EF) and receiver-operator-characteristic (ROC) plots as well as other early performance metrics.



## ■ INTRODUCTION

Ligand-based shape matching approaches have become well established as important and popular virtual screening (VS) techniques. Nonetheless, despite their relative success, many authors have discussed how to choose the initial query compounds and which of their conformations should be used.<sup>1,2</sup> These questions gain importance when dealing with “difficult” targets, such as targets which bind multiple ligands in different subsites. Furthermore, it is increasingly the case that pharmaceutical companies have multiple ligands for a given target and these may bind in different ways to the same pocket. However, traditional shape matching approaches normally use just one conformation of a compound as the query, but it is not known *a priori* if this is the correct query to use to screen an entire database. For example, other compound families could also be active for a given target, but they might only be found in the database if a different query conformation is used. In other words, conventional VS assumes there is only one binding mode for a given protein target. This may be true for some targets, but it is not true in all cases. Several recent studies have described proteins which bind different ligands in different ways. For example, multiple binding sites and multiple binding modes have been reported for

CCR5,<sup>3</sup> CXCR4,<sup>4</sup> CDK2,<sup>5</sup> LXR $\beta$ ,<sup>6</sup> the integrins  $\alpha 1\beta 1$  and  $\alpha 2\beta 1$ ,<sup>7</sup> VEGFR2,<sup>8</sup> FXA,<sup>9</sup> ACHE,<sup>10,11</sup>  $\gamma$ -secretase,<sup>12</sup> Oncoprotein c-Myc,<sup>13</sup> ALR2,<sup>14,15</sup> P38,<sup>16</sup> and  $\beta$ -secretase.<sup>17,18</sup>

There is no doubt that choosing a good query can improve shape-based VS performance. For example, Kirchmair et al.<sup>2</sup> found that using the center molecule of a set of active compounds gave better VS performance than using a single crystallographic ligand as the query. Moreover, they showed that exploiting structural information of several different active compounds further increases hit retrieval rates. We recently introduced the notion of spherical harmonic (SH)-based “consensus shapes” to cluster and classify known CCR5 ligands.<sup>19</sup> This approach allows one or more “pseudo-molecules” to be created and used as VS query structures. In a previous study on some 15 diverse families of CCR5 inhibitors which could not all be superposed together, we found that the ligands may be clustered into four main superconsensus (SC) families, and we predicted that these SCs bind within three subsites in the CCR5 extra-cellular pocket.<sup>20</sup> These predictions were consistent with experimental site-directed

**Received:** December 11, 2010

**Published:** May 23, 2011

**Table 1.** Summary of the Different Queries Used against the DUD Targets

method/query	explanation
PARAFIT_B	PARAFIT using the bound crystallographic ligand in the DUD target complexes.
PARAFIT_CM	PARAFIT using a SH consensus molecule calculated from all actives.
PARAFIT_C1_CM, PARAFIT_C2_CM, and PARAFIT_C3_CM	PARAFIT using three representative consensus molecules for each target, calculated from three shape-based clusters of the conformations of the DUD ligand sets (clusters C1, C2, and C3 consensus molecules).
PARAFIT_RCM	PARAFIT using the real center molecule, i.e. the real molecule whose SH surface is closest to the consensus shape.
PARAFIT_C1_RCM, PARAFIT_C2_RCM, and PARAFIT_C3_RCM	PARAFIT using the three real center molecules of clusters C1, C2, and C3.
PARAFIT_SHEF_C	Using as the PARAFIT query the molecule which best fits the target pocket as calculated by SHEF.
ROCS_B	The bound ligand conformation used as a ROCS query.
ROCS_RCM	The real center molecule from PARAFIT used as ROCS query.
ROCS_C1_RCM, ROCS_C2_RCM, and ROCS_C3_RCM	The three real center molecules from PARAFIT for clusters C1, C2, and C3 used as ROCS queries.
ROCS_SHEF_C	The best SHEF molecule that fits the pocket used as ROCS query.

mutagenesis information and other computational studies. This suggested that consensus clustering could offer a straightforward way to understand how multiple ligands might distribute themselves within a given binding site. In order to explore further the utility of this approach, we subsequently applied our clustering approach to the 40 protein–ligand targets of the DUD data set.<sup>21</sup>

Here, we show three main applications: using shape clustering to identify promiscuous targets (targets which may bind different ligands in different ways) and promiscuous ligands (ligands which may bind to more than one protein target), using consensus shapes to understand promiscuous targets, and using consensus shapes to choose the right query in shape-based VS.

Regarding the first application, our results from clustering the active ligands in the DUD data set using PARASURF<sup>22</sup> and PARAFIT<sup>23,24</sup> show that in some cases the ligands for a given target are split into two subgroups which could suggest they bind to different subsites of the same target. On the other hand, in other cases, our clustering approach sometimes groups together ligands from different targets, and this suggests that those ligands could be promiscuous. The all-against-all DUD cross-docking experiment of Huang et al.<sup>21</sup> also indicates that some ligand families might bind to more than one target. Because ligand-based clustering is much faster than protein–ligand docking, it would be very useful to be able to use clustering techniques to identify such cases and hence avoid the expense of performing all-against-all docking calculations.

With regard to the second application, here we present a new protocol to understand difficult VS targets and to reveal promiscuity based on consensus shape clustering. For each target, we initially calculate three clusters of ligands based on chemical fingerprints and then use the VS profiles to detect promiscuity. We use three clusters on the assumption that the actives for a given target might split into up to three main groups and that it is unlikely that a target will have more than three subsites. Potential promiscuous targets which are detected in this way are then explored by consensus shape clustering. Here we apply this approach to each of the 40 DUD targets, and we analyze in detail two detected multiple binding site targets (P38 and ALR2). We

also report on the impact of the query conformation on the performance of shape-based screening of these promiscuous targets and the potential gain in performance by using consensus shapes calculated in different ways.

With respect to the third application, in a previous study using the DUD targets, we showed that the performance of 2D and 3D ligand-based VS methods can vary considerably for different targets according to the area under of the curve (AUC) of receiver-operator-characteristic (ROC) plots.<sup>25</sup> For example, some targets showed very good VS performance ( $AUC \geq 0.8$ : COX2, RXR-ALPHA, ER-AGONIST, and SAIHH), whereas other targets showed essentially random VS performance ( $AUC \sim 0.5$ : CDK2, COX1, PR, THROMBIN, VEGFR2, ACE), and some even showed worse than random performance ( $AUC < 0.5$ : ALR2, COMT, TRYPSIN, P38, and PDGFRB). Giganti et al.<sup>26</sup> found a similar variation in the screening performance of the DUD targets. Several targets showed poor VS performance, mainly those with large binding pockets such as P38, where it is difficult to accommodate all ligand conformations. As it is known that some ligands can adopt multiple binding modes (e.g., the CDK2, FXA ligands) or can bind to multiple binding subsites in a given target pocket (e.g., the P38, ALR2, VEGFR2, ACHE targets), it is unrealistic to expect that a single VS query can select all the active compounds in such cases. Therefore, given that 3D ligand-based VS methods do not perform as well as expected even when multiple conformations for each database compound are used,<sup>25</sup> we wished to explore the use of consensus shapes to construct more effective VS queries.

Kirchmair et al. previously obtained better VS performance by using the center molecule of the compound set or by using several different active compounds as the query. Here, we extend this approach by using the notion of SH consensus pseudomolecules. We provide detailed analyses of the utility of each type of VS query against the DUD data set using both PARASURF/PARAFIT and ROCS,<sup>27</sup> and we compare the results obtained with the receptor-based MSSH/SHEF<sup>28,29</sup> and GOLD<sup>30</sup> docking approaches. Commonly reported statistics such as enrichment factors (EF) and ROC plots as well as early performance metrics have been calculated to analyze the VS performance of the different queries explored.

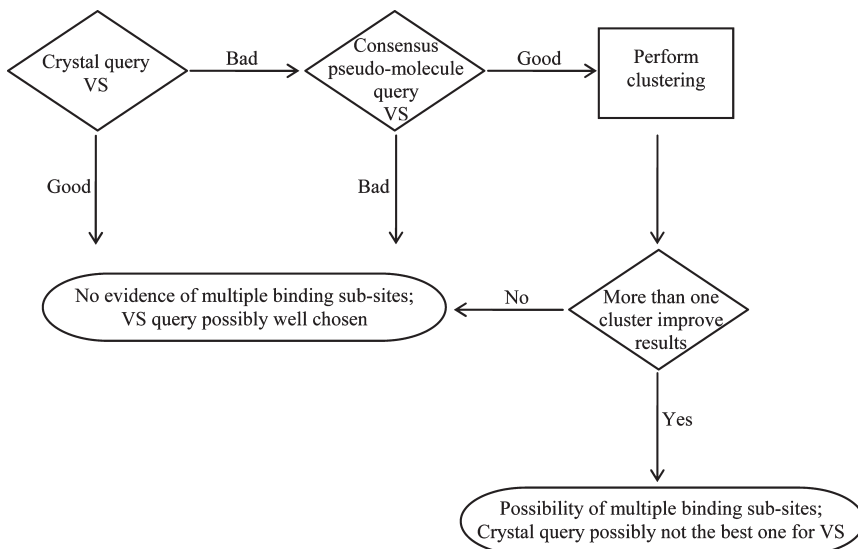


**Figure 1.** Flowchart for using the consensus clustering protocol to explore multiple binding sites.

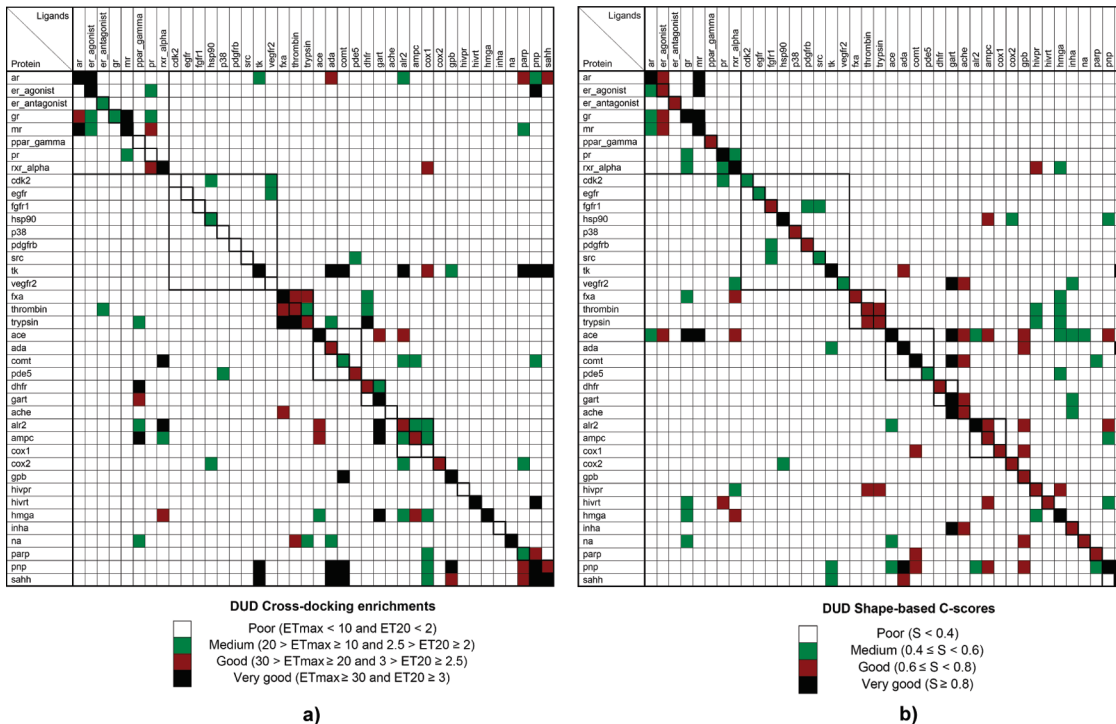


**Figure 2.** Comparing cross-docking and cross-shape matching of the DUD data set. a) Cross-docking enrichments reproduced from Huang et al.<sup>21</sup> b) Shape-based C-Scores from the all-against-all shape clustering calculation. A C-Score threshold of 0.1 was selected to emphasize the overall similarity to the cross-docking experiment. C-scores are grouped into four bins: very good (C-Score > 0.8) corresponds to black, good ( $0.6 \leq \text{C-Score} < 0.8$ ) corresponds to red, medium ( $0.4 \leq \text{C-Score} < 0.6$ ) corresponds to green, and poor ( $\text{C-Score} < 0.4$ ) corresponds to white. For example, when ar is over the threshold, the sum of the normalized number of ligands of er\_agonist over the threshold for all the clusters is between 0.6 and 0.8, shown in red in the table. When ar is over the threshold, the sum of the normalized number of ligands of mr over the threshold for all the clusters is over 0.8, shown in black in the table.

## METHODS

**SH Consensus Shape Matching.** We used the PARASURF and PARAFIT modules<sup>31</sup> to calculate and superpose SH molecular surfaces. PARASURF calculates molecular shape and electronic properties from semiempirical quantum mechanics theory

and encodes these properties as SH expansions.<sup>22</sup> Surface shapes are represented as radial distance expansions of the molecular surface with respect to a selected harmonic coordinate origin, which is normally set equal to the molecular center of gravity.<sup>24</sup> This allows an entire molecular surface shape to be captured using a Fourier-like polynomial expansion, and pairs of such

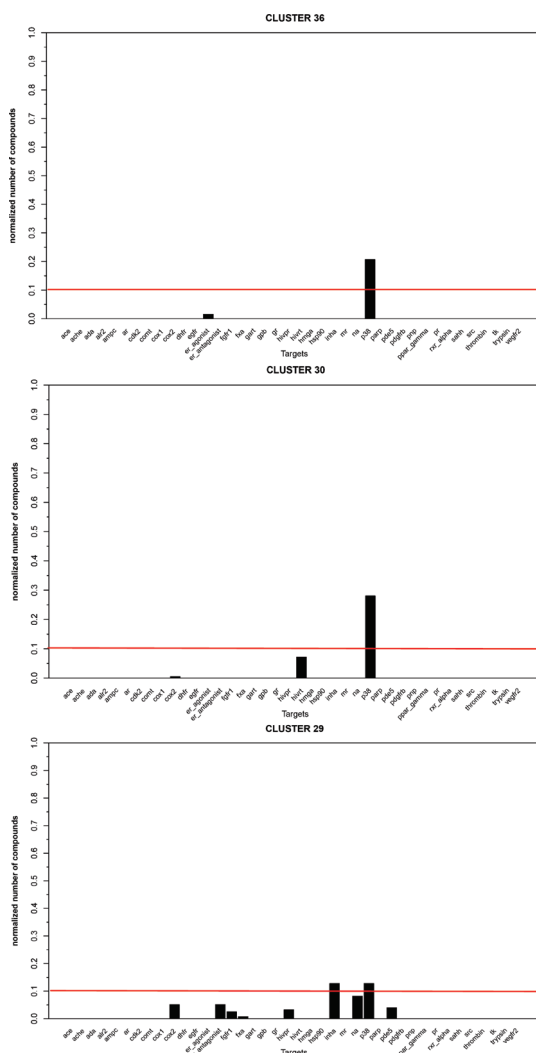


**Figure 3.** All-against-all DUD consensus clustering showing the P38 ligands split into three main clusters (C29, C30, C36). The black bars give the C-Score for each of the 40 DUD targets found in a particular cluster.

expansions can be compared rapidly using fast Fourier transform techniques.<sup>23</sup> It is also straightforward to construct the average or “consensus” shape of a group of molecules by calculating the average of their SH expansions.<sup>19</sup> This consensus shape-based representation can be used to capture the essential 3D shape features of several known high-affinity ligands and to encode them in the form of a single representative pseudomolecule which may be used as a VS query.

**The Directory of Useful Decoys (DUD).** The DUD data set<sup>21</sup> currently contains a total of 2,950 active compounds against a broad variety of therapeutic targets, along with 36 similar “decoy” molecules for each active compound. It was first built to assist the validation of docking protocols, and recent versions have become standard data sets for the evaluation of both structure-based and ligand-based VS methods.

The DUD data set was screened for duplicates using MOE.<sup>32</sup> For each of the 40 targets in the data set, the known actives and the target-specific decoys were used to compare the performance of different queries in 3D shape-based and docking methods. Several trial queries, including the crystallographic ligand conformation,

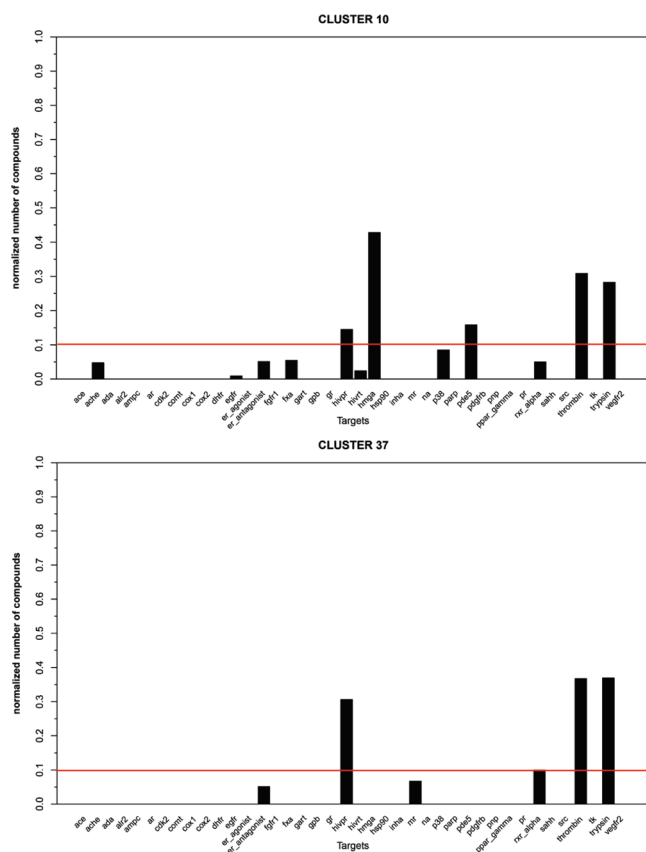


**Figure 4.** All-against-all DUD consensus clustering showing the THROMBIN ligands grouped with the TRYPSIN, HIVPR, and HMGA ligands. The black bars give the C-Score for each of the 40 DUD targets found in the clusters where THROMBIN appears (C10 and C37). Using a C-Score of 0.1 as threshold suggests the THROMBIN ligands might cross-dock with TRYPSIN, HIVPR, and HMGA.

were compared. Although the choice of ionization states and tautomers can affect VS results,<sup>33</sup> in this study the molecular structures were used in their default form.

#### Predicting Promiscuity Using Ligand Shape Clustering.

ParaFit was used to perform an all-against-all shape comparison for all of the active ligands in the DUD data set, and the resulting similarity matrix of 2950 ligands was clustered into 40 clusters using Ward’s hierarchical clustering. In order to calculate the relative extent to which a set of target-specific ligands are grouped together, we define a cluster score or “C-score” as

$$C_L^c = \frac{n_L^c}{N_L} \quad (1)$$

where  $N_L$  is the total number of ligands associated with a given target (which we call a “ligand set”), and  $n_L^c$  is the number of ligands from ligand set  $L$  found in cluster  $c$  ( $c = 1, 2, \dots, 40$ ). To determine whether certain targets or groups of ligands are promiscuous, we set a C-Score threshold of 0.1 in order to highlight a similar number of predicted interactions to those in the cross-docking experiment of Huang et al.<sup>21</sup> In other words, when for a given ligand set one or some of the clusters are found to contain multiple groups of ligands belonging to this ligand set and also some other ligand sets each over the threshold, then the target associated with this ligand set is considered to be a

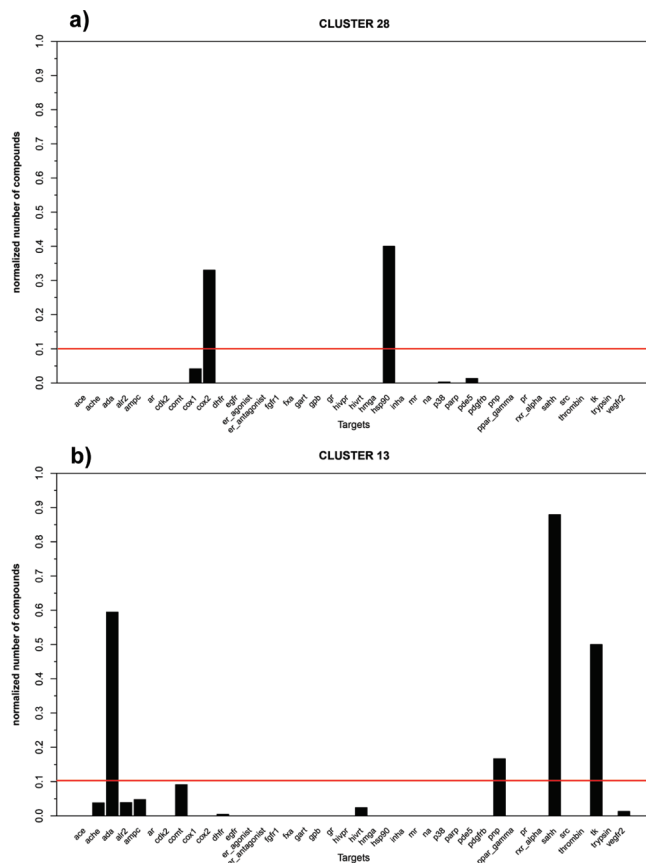


**Figure 5.** All-against-all DUD consensus clustering suggesting that (a) the COX2 ligands might cross-dock with HSP90 ligands and (b) the SAHH ligands might cross-dock with the TK and ADA targets.

promiscuous target. Conversely, if the members of a given ligand set appear in multiple clusters with C-Score >0.1, those ligands are considered to be potentially promiscuous.

**Shape-Based Virtual Screening.** The utility of using SH consensus shapes as VS queries was compared with the default PARAFIT 09<sup>23</sup> and ROCS 2.4.<sup>27</sup> shape-based approaches and also with two other methods which take into account the receptor, i.e. one shape-based docking (MSSH<sup>28</sup>/SHEF<sup>29</sup>) and one conventional docking method (GOLD 3.2<sup>30</sup>). MSSH/SHEF is a fast SH-based protein–ligand docking algorithm for matching ligand surface shapes to protein binding pockets. The root mean squared deviation (rmsd) between corresponding pairs of surface sample points is used as the scoring function, and a genetic algorithm is used to find the rotation of each ligand which minimizes this distance.

Here, all programs were used with default parameters, and all approaches used 10 conformations per database compound except for PARAFIT which used only the original DUD active conformations, and GOLD which generates its own conformations. ROCS and MSSH/SHEF used conformations generated by OMEGA<sup>34</sup> with a default energy window for acceptable conformers of 10 kcal/mol above the ground state and a rmsd cutoff of 0.5 Å. The scoring functions used were the PARAFIT shape Tanimoto score, the ROCS Combo score, the rmsd score in MSSH/SHEF, and the GOLD GoldScore. Table 1 summarizes the various algorithms and query structures that were evaluated.

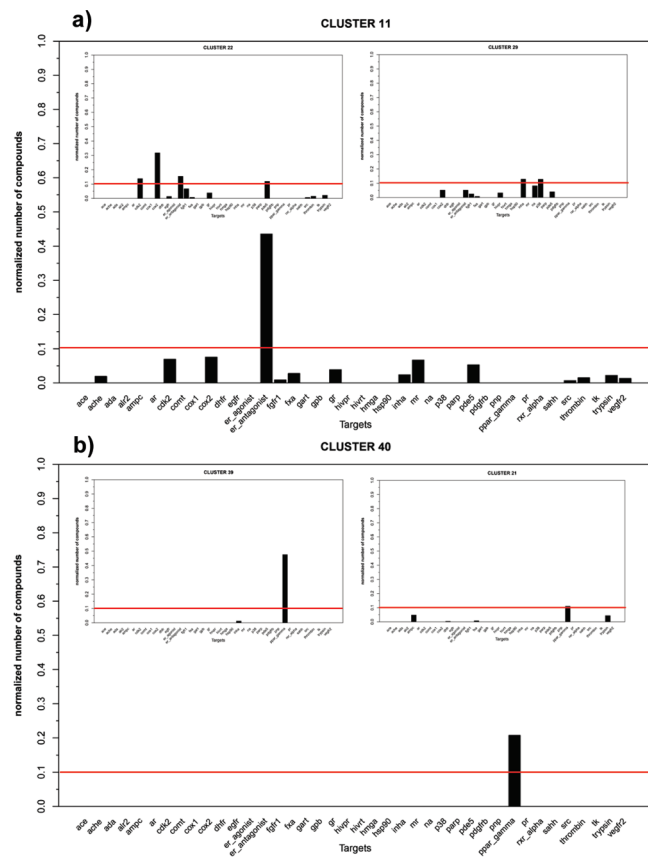


**Figure 6.** All-against-all DUD consensus clustering suggesting that (a) the ER-ANTAGONIST ligands and (b) the PPAR-GAMMA ligands probably do not cross-dock with other targets.

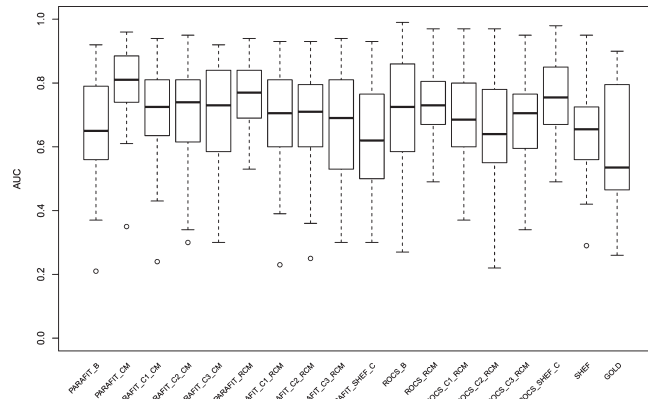


**Figure 7.** Box plot summaries of each VS method/query combination evaluated in the present study for the 40 DUD targets. The method/query combinations on the horizontal axis are described in detail in Table 1. The dashed error bars represent standard deviations. The bold black line represents the median AUC. It can be seen that the median AUC is highest for the PARAFIT consensus pseudomolecule query.

**Performance Metrics.** Finding new approaches which can select actives in the top-scoring fraction of the database can reduce costs in laboratory-based drug screening. Hence, several different metrics for assessing query performance in DUD shape-based VS were studied, ranging from commonly used statistics to those that highlight early performance. The common metrics

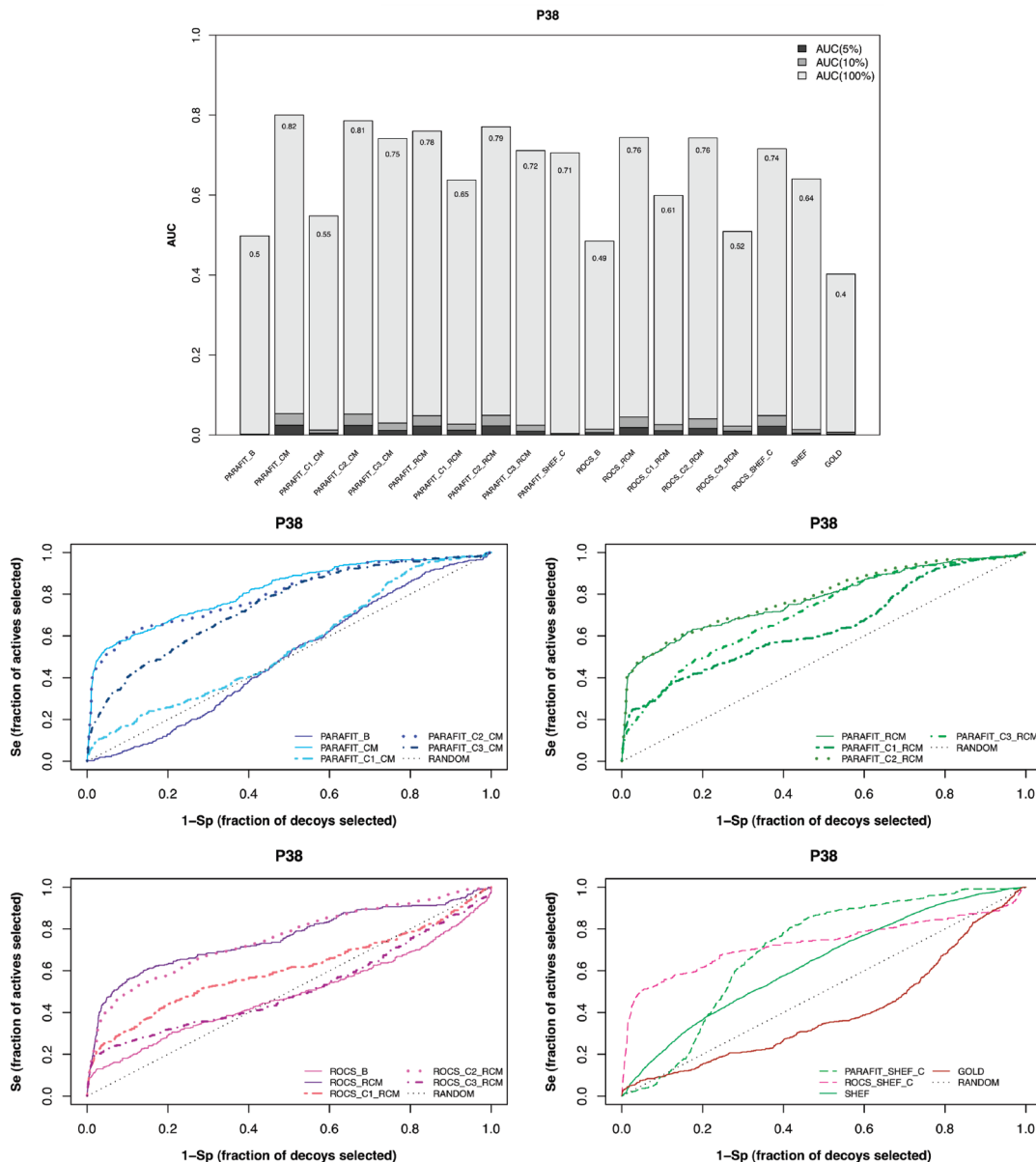


**Figure 8.** Bar graph and ROC plots for P38 VS. This figure shows that using the all-ligand consensus shape greatly improves VS performance. All three clusters (PARAFIT\_C1\_CM, PARAFIT\_C2\_CM, and PARAFIT\_C3\_CM) individually improve the performance compared to both the PARAFIT pseudomolecule and PARAFIT and ROCS real consensus molecule. The main improvement is due to cluster C2, but clusters C1 and C3 show a similar trend. This suggests that P38 has more than one binding site.

used here are the AUC of ROC plots,<sup>35</sup> the enrichment factor (EF),<sup>36</sup> and normalized enrichment factor (EFrel)<sup>37</sup> at 1%, 5%, and 10% of database screened. The early performance metrics are Boltzmann-Enhanced Discrimination of ROC plots (BAROC<sup>36</sup> and BEDROC<sup>38</sup>) and Normalized Sum of Log Ranks (NSLR).<sup>25</sup>

**Consensus Clustering: Detecting and Analyzing Multisite Pockets.** We use consensus clustering to detect candidate promiscuous targets by considering only the known active ligands for each target. First, we assume that if the crystallographic query gives poor VS performance, the target could have multiple binding subsites, and therefore that repeating the VS using consensus pseudomolecules is worth considering. If this does not substantially improve the VS results, we presume there are probably not multiple binding subsites and the query could be already well chosen, but the VS performance is poor for other reasons, e.g. the

crystallographic ligand is very different in chemistry or in size from the ligand set. On the other hand, if using a consensus pseudomolecule substantially improves the VS results, the crystallographic ligand was not the best one for the VS, and we presume that ligand-based clustering should be further explored.

In such cases, we cluster the active compounds of each target to be considered into three groups using Ward's hierarchical clustering of chemical fingerprints<sup>39</sup> as implemented in the JKluster module of JChem.<sup>40</sup> We then use PARAFIT to generate consensus pseudomolecules for each of the three clusters for use as trial VS queries with the target-specific ligands and decoys. If at least two of the consensus shapes give better VS performance than the crystallographic ligand, we treat this as evidence that the target has multiple binding subsites. Here, two such cases were found (P38 and ALR2), and these were analyzed in further detail

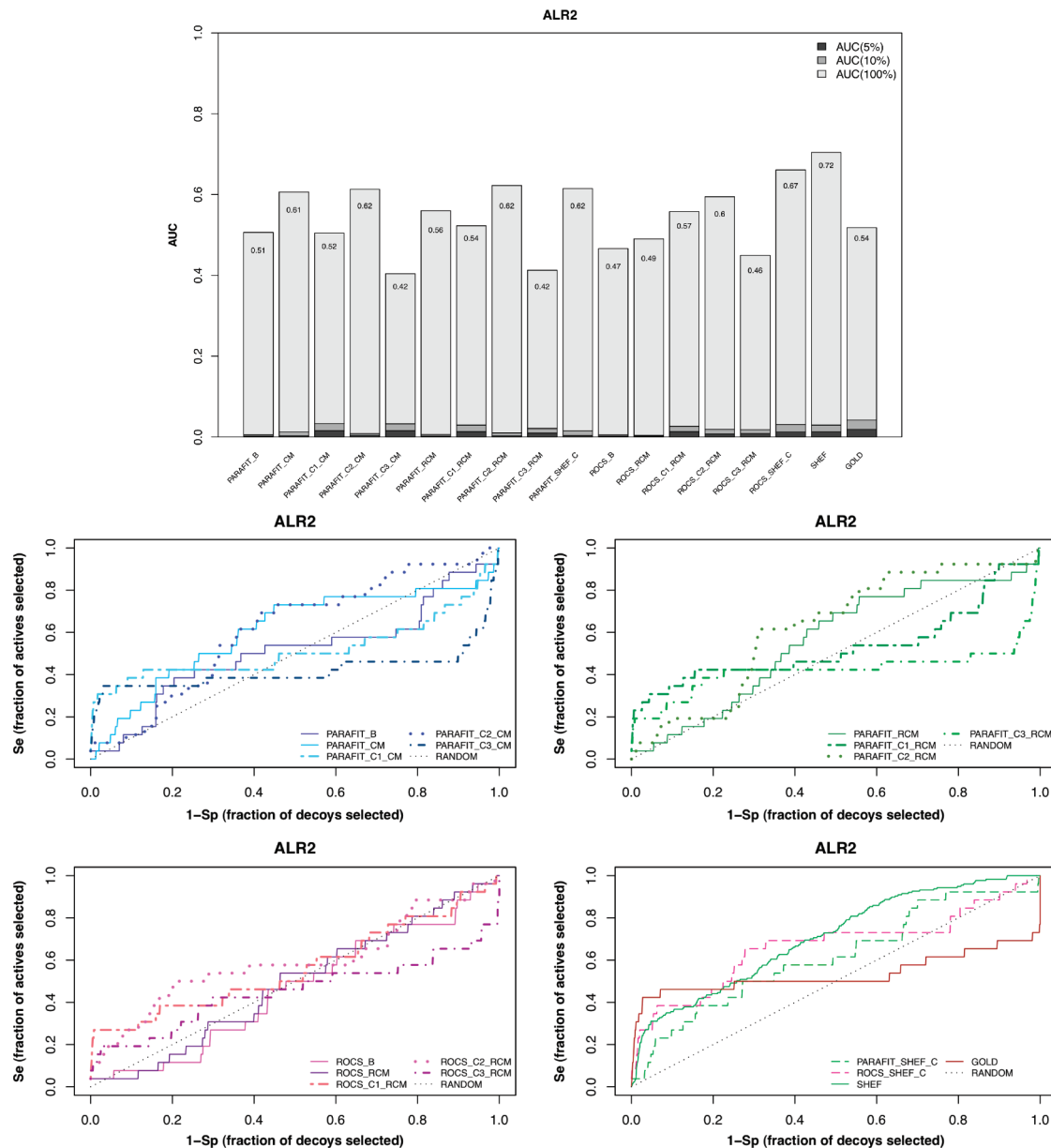


**Figure 9.** Bar graph and ROC plots for ALR2 VS. This figure shows that using a consensus shape and splitting the ligands into clusters both improve VS performance. This suggests that ALR2 is a promiscuous target.

by reclustering. For these cases, Ward's hierarchical clustering of chemical fingerprints was performed using Kelley's method<sup>41</sup> to find the optimal number of clusters, and SH consensus shapes were calculated for each of the groups found. An all-against-all SH comparison of each consensus shape was calculated using PARAFIT, and the resulting pairwise Tanimoto similarity scores were used to calculate consensus superclusters (SC) using a further round of hierarchical clustering. SC pseudomolecules were rigidly docked into the target structures using blind Hex docking with default search parameters.<sup>23</sup> In each case, the pseudomolecule was initially placed outside the receptor pocket. Binding pocket subsites were proposed from the resulting docking poses. The flowchart shown in Figure 1 summarizes this protocol for analyzing multiple binding sites.

It is worth mentioning that here we have used Chemaxon's chemical fingerprint similarity measure for preclustering, and we

use those clusters for further processing. However, using other molecular properties (e.g., size) for preclustering could be more suitable to help in the interpretation of the promiscuity results. For example, since shape complementarity is an essential feature for molecular recognition, the molecular shape should provide a good way to characterize and precluster known ligands.

## ■ RESULTS

**All-against-All Shape Clustering vs Cross-Docking.** Figure 2 compares the docking-based and ligand-based clustering of the DUD ligands using a C-Score threshold of 0.1. In the ideal case, all of the ligands for each target would appear in a separate cluster, and each cluster would correspond to one target. However, in practice, the ligands are grouped much less evenly than this, and our results show that in some cases the ligands for a given target are split into

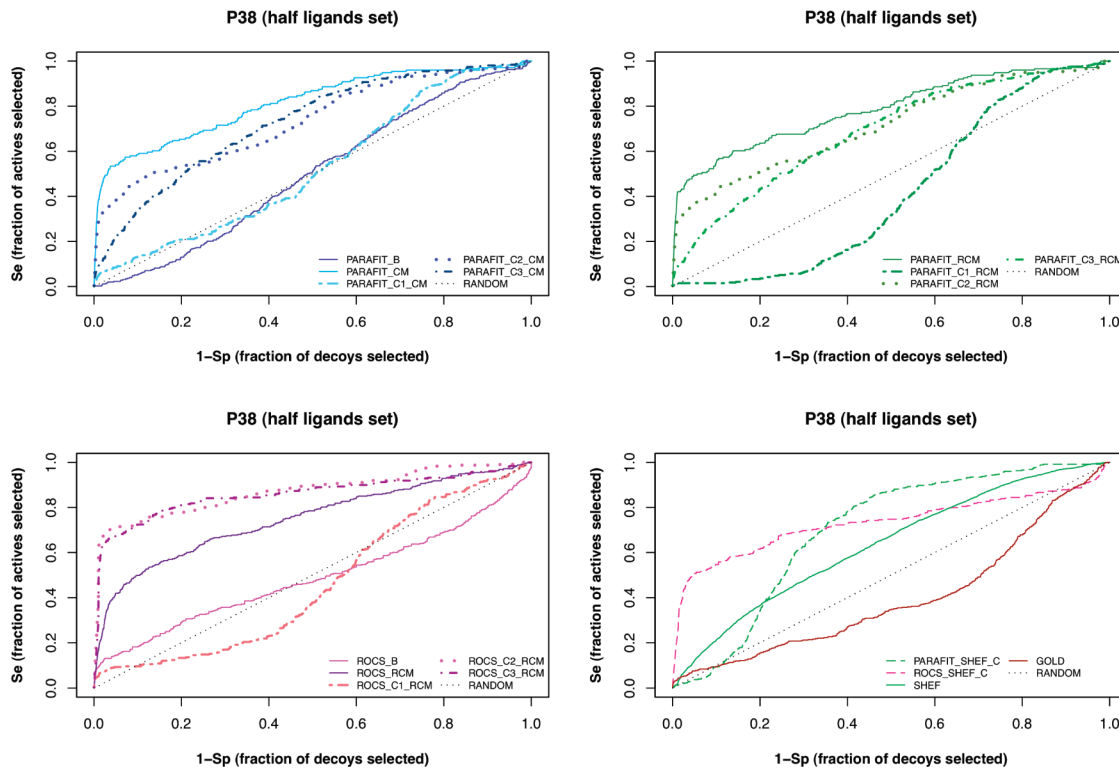


**Figure 10.** ROC plots of the leave-some-out validation of the consensus shape approach applied to the P38 target. Half of the P38-specific ligands were used to build the consensus shape query and the remaining P38-specific ligands and decoys for VS.

two or three main subgroups (e.g., the ligands for P38 form three clusters, see Figure 3).

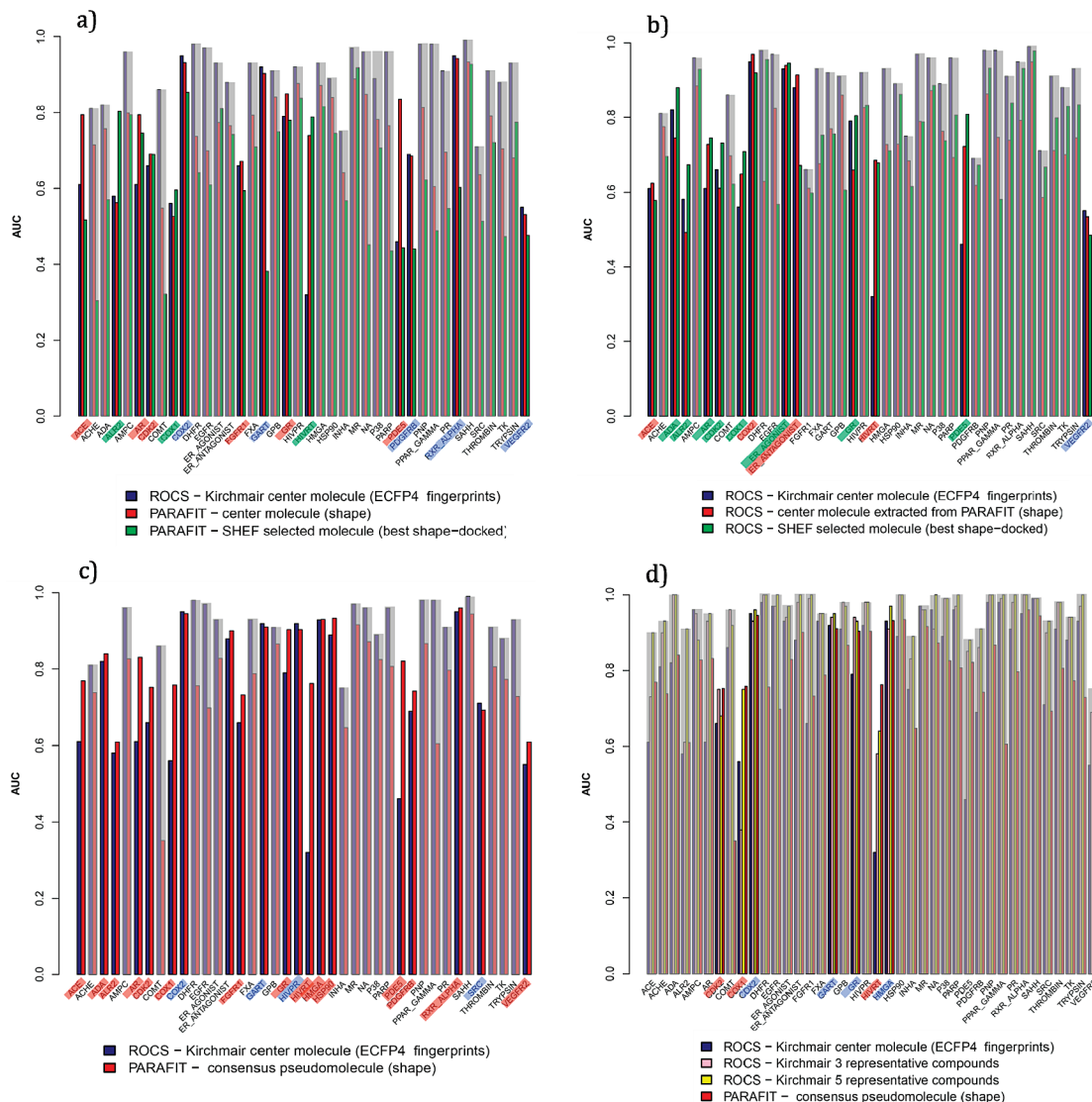
Figure 4 shows that the thrombin ligands appear in two clusters (C10 and C37) together with members of other ligand sets with a C-Score above the threshold. Using a C-Score threshold of 0.1 suggests that the thrombin ligands might cross-dock to the HIVPR, HMGA, and TRYPSIN targets (see Figure 2b). Considering clusters C10 and C37 together, the overall C-Score for the HIVPR ligands is  $0.15$  (C10) +  $0.35$  (C37) =  $0.5$ , and the overall C-Score for the TRYPSIN ligands is  $0.3$  (C10) +  $0.4$  (C37) =  $0.7$ . Similarly, a C-Score of  $0.45$  is found for the HMGA ligands and  $0.15$  for the PDES ligands. Although one should expect the diagonal of the cross-shape matching matrix to be black (corresponding to very good C-Score values in Figure 2b), this does not always happen because only those members of a ligand set above the threshold are summed (e.g., the overall C-Score for thrombin ligands is  $0.35$  (C10) +  $0.4$  (C37) =  $0.75$ , which is represented in red in the diagonal of the table in Figure 2b). Hence, other colors such as green (representing medium C-Score values) or red (representing good C-Score values) in the diagonal show targets for which some of their ligands are assigned to other clusters.

Figure 5 shows examples of targets which are found to be promiscuous according to the chosen C-Score threshold. Figure 5a shows that cluster C28 mainly groups together ligands for the COX2 with HSP90 (C-Score =  $0.45$ ). Figure 5b shows C13, grouping together ligands for SAHH with TK (C-Score =  $0.45$ ), and ADA (C-Score =  $0.60$ ). Figure 6 shows examples of targets which are predicted not to be promiscuous according to the chosen C-Score threshold. Figure 6a shows that the ER-ANTAGONIST ligands are not grouped with other ligand sets, or if they are grouped, the C-Score for these ligands is typically below

the threshold. A similar trend is seen for the PPAR-GAMMA ligands (Figure 6b), which are also not grouped with other ligand sets according to the chosen threshold.

The above examples agree with the cross-docking results of Huang et al.<sup>21</sup> which are summarized in Figure 2a. Comparing Figure 2a and Figure 2b, it can be observed that shape clustering gives comparable results to cross-docking. However, while all-against-all shape clustering takes about 8.5 CPU-hours, cross-docking takes several CPU-months (from 20 h to 12 days per target). This suggests shape clustering techniques can identify possible cross-docking targets without the expense of all-against-all docking calculations.

**DUD Shape-Based VS.** Figure 7 summarizes the overall VS performance of each method/query combination tested on the 40 DUD targets. It can be observed that the PARAFIT consensus shape query (PARAFIT\_CM) gives the best AUC values, showing a high median and a small standard deviation between values, suggesting robustness of the approach. However, PARAFIT and ROCS using the crystallographic ligand (PARAFIT\_B and ROCS\_B) have larger standard deviations which implies that the crystallographic ligand is well-suited for some targets but not for others. The consensus pseudomolecules of each of the three clusters also have respectable AUC performance, but they have higher standard deviations. This is presumably because it is not always appropriate to split ligands into subsets. It is also worth noting that both PARAFIT and ROCS using the real consensus molecule (PARAFIT\_RCM and ROCS\_RCM) give good performance for all targets with small standard deviations. The AUC values obtained are better than those of the real consensus molecules of each of the three clusters C1, C2, and C3. This confirms that SH consensus clustering provides a good way to select a central molecule for a set of ligands. It can be also seen



**Figure 11.** AUC comparison of VS query performance. AUC values obtained when screening the DUD database using as the query: a) Kirchmair's center molecule of each target-specific ligands set in ROCS (blue), PARAFIT real consensus molecule (red), and PARAFIT using the SHEF-selected molecule (green); b) Kirchmair's center molecule of each target-specific ligands set in ROCS (blue), ROCS real consensus molecule (red), and ROCS using the SHEF-selected molecule (green); c) Kirchmair's center molecule of each target-specific ligands set in ROCS (blue), PARAFIT consensus pseudomolecule (red); d) Kirchmair's center molecule of each target-specific ligands set in ROCS (blue), Kirchmair's three representative compounds of each actives set used in ROCS (beige), Kirchmair's five representative compounds of each actives set used in ROCS (yellow), PARAFIT consensus pseudomolecule (red). Gray bars highlight the targets for which Kirchmair's center molecule used as the query retrieves the best performance. Names in red highlight when the center/real molecule (in a,b) or consensus pseudomolecule (in c,d) extracted from PARAFIT performs as the best query. Names in green highlight when SHEF-selected molecule as query performs the best. Names in blue highlight when the center/real molecule (in a,b) or consensus pseudomolecule (in c,d) extracted from PARAFIT gives very similar results to Kirchmair's center molecule in ROCS.

from Figure 7 that GOLD gives the lowest median AUC with the largest standard deviation. Indeed, SHEF shape-based docking performs substantially better than conventional GOLD docking. Furthermore, using the SHEF-selected molecule as a query gives very good results with ROCS but somewhat worse results with PARAFIT. Overall, these results also show that ligand-based approaches give better VS performance than SHEF and GOLD docking. However, using a query conformation extracted from SHEF docking improves the VS performance of ligand-based approaches.

#### Choosing the Right Query in DUD Shape-Based VS.

ROC plots and AUC bar graphs were made for each of the 40 DUD

targets to compare the VS performance of the various queries. Individual plots, AUC bar graphs, and details of the statistics calculated are available in the Supporting Information. Here, we focus on some examples for which conventional shape-based VS gives poor results (COMT, TRYPSIN, PDGFRB, P38, ALR2) and others for which it performs well (COX2, SAHH, RXR-ALPHA, ER-AGONIST). For example, the Supplementary ROC plot and AUC bar graph for the COMT target show that the pseudomolecule constructed from consensus cluster C2 gives better results than the crystallographic ligand. The AUC also improves when using the real consensus molecule as the query with both PARAFIT and ROCS. Since the consensus shape

**Table 2.** AUC Values Obtained Using Various PARAFIT Queries against the Given DUD Targets

target	PFT_B	PFT_CM	PFT_C1_CM	PFT_C2_CM	PFT_C3_CM	promiscuous prediction
CCR5	0.594	0.866	0.785	0.905	0.505	✓
ALR2	0.508	0.609	0.520	0.617	0.419	✓
COMT	0.371	0.351	0.508	0.674	0.378	
TRYPSIN	0.207	0.728	0.740	0.639	0.639	
PDGFRB	0.448	0.742	0.667	0.678	0.579	
P38	0.498	0.825	0.552	0.809	0.753	✓
CDK2	0.524	0.752	0.661	0.769	0.510	✓
COX1	0.574	0.758	0.652	0.716	0.581	
PR	0.591	0.797	0.752	0.741	0.676	✓
THROMBIN	0.623	0.806	0.426	0.808	0.775	✓
VEGFR2	0.598	0.609	0.472	0.556	0.629	
ACE	0.572	0.769	0.804	0.452	0.642	✓

seems to capture important features of the known actives, it is therefore perhaps not surprising that the real molecule closest to the consensus provides a very good VS query.

The Supplementary ROC plot and AUC bar graph for TRYPSIN target show that the central molecules of clusters C1 and C3 also provide better queries than the crystallographic ligand in both PARAFIT and ROCS. Here, SHEF also gives good results, and the SHEF-selected query molecule in both PARAFIT and ROCS also performs well. In this case, the crystallographic query is chemically different from the ligand and decoy sets. This might explain its poor performance both in PARAFIT and ROCS screening. A similar trend is seen in the PDGFRB Supplementary ROC and AUC plots, in that the central molecule of cluster C2 seems to be a better query than the crystallographic one for both PARAFIT and ROCS. Here the crystallographic PDGFRB ligand is also appreciably different from the other ligands.

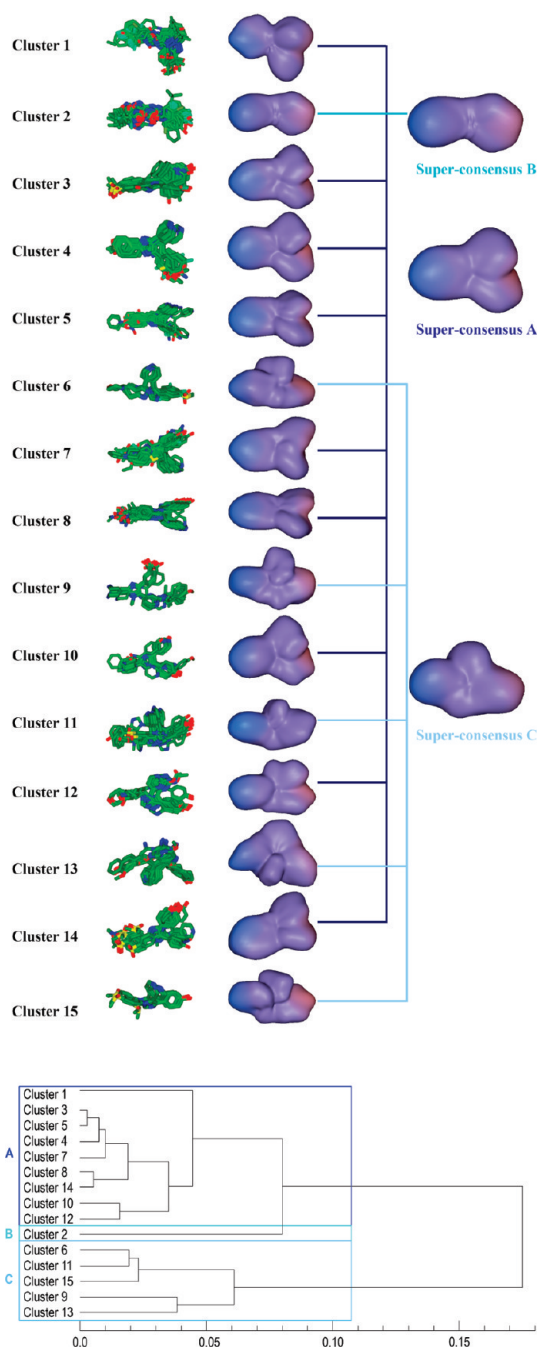
Figure 8 shows that using the all-ligand consensus shape for P38 greatly improves VS performance. All three clusters (PARAFIT\_C1\_CM, PARAFIT\_C2\_CM, and PARAFIT\_C3\_CM) individually improve the performance compared to both the PARAFIT consensus molecule and PARAFIT and ROCS with the real consensus molecule. The main improvement is seen for cluster C2, but clusters C1 and C3 show a similar trend. As proposed above, this suggests that P38 is a promiscuous target. Overall, these results support the notion that using only one representative ligand to screen a database of actives is not the best choice to achieve good VS performance for such targets, and it is worthwhile to calculate shape-based clusters of the conformations of multiple actives in order to identify the best VS query to use. The bar graph in Figure 8 also shows that the consensus pseudomolecule and its corresponding real consensus molecule are also good queries at the first percentages of database screened with better 5% and 10% AUCs than the crystallographic ligand. The ROC plots clearly show the poor VS performance of the crystallographic query and the considerable improvement that is obtained by using the C2 consensus pseudomolecule and the real consensus molecule in both PARAFIT and ROCS.

Figure 9 shows the bar graph and ROC plot for the ALR2 target, which also gives poor VS performance when using the crystallographic ligand as the query. It can be seen that the all-ALR2 ligand consensus molecule provides a good query, mainly due to the ligands belonging to cluster C2. The same trend can be

seen when using the PARAFIT-selected real molecule as the query for both PARAFIT and ROCS. Hence, in this case, the real consensus molecule in cluster C2 could be a better query than the crystallographic one. SHEF shape-based docking also performs well, and the SHEF-selected real molecule is also found to be a good query with both PARAFIT and ROCS. Although the VS improvement seen when using the ALR2 consensus shapes is lower than for P38, a similar trend is observed. However, even though the ligand set is similar to the crystallographic ligand, using a consensus shape and using consensus clusters both improve VS performance. This unexpected result could therefore be providing a clue that this target is promiscuous. Hence, target promiscuity was also explored, as described below.

The Supplementary ROC plot and bar graph for the COX2 target show that good VS results are obtained (especially by ROCS) using the crystallographic ligand as the query. It is therefore difficult to construct a better query using our protocol. However, with PARAFIT, the PARAFIT\_CM often gives better VS performance than the crystallographic ligand and any of the individual clusters. The same is true for the SAHH target. However, for RXR-ALPHA, which also gave good VS results using the crystallographic ligand as the query, all queries perform comparably to the crystal structure except cluster C1 in PARAFIT, cluster C2 in ROCS, and the SHEF-selected molecule in PARAFIT. The same is seen for the ER-AGONIST target. In this case, some queries improve the crystallographic ligand results, but using cluster C1 as the query is worse than using the crystal query (see the Supporting Information). Overall, these results show that for cases where ligand-based VS is successful (e.g., COX2, RXR-ALPHA, ER-AGONIST), using consensus shapes as queries usually gives better performance than conventional shape-based docking methods.

**Leave-Some-Out Validation.** It could be argued that calculating a consensus molecule using a large number of known actives is in some way “over-training” the query. In order to explore the robustness of the consensus shape approach regarding this proposition, leave-some-out validation was applied to the P38 target, using half of the P38-specific ligands to build the consensus shape query, and using the remaining P38-specific ligands and decoys for VS. Similarly, for each consensus cluster, half of the P38 ligands in the cluster were used to build the consensus query and the remainder were placed among the P38 decoys. Figure 10 shows that the results obtained are similar to using all of the ligands to build the consensus queries.



**Figure 12.** Molecular superpositions and consensus shapes of the fifteen Ward's clusters used to calculate the final P38 SH SC shapes. The dendograms show the initial fifteen P38 groups clustered using Ward's clustering of SH distances between the consensus surface shapes of each group. The three main SC groups, labeled A, B, and C, are highlighted.

Cluster C1 especially worsens the AUC values with respect to constructing the query from all actives, especially compared to using the real consensus molecules (PARAFIT and ROCS). For ROCS, cluster C1 worsens AUC values. However, clusters C2 and C3 substantially improve VS performance. In other words, using fewer actives to form the consensus clusters improves VS performance for two out of three clusters. This implies that using all available actives to form a single consensus is not overtraining and could even be detrimental.

**Comparison with Previous Work.** To optimize DUD target queries using ROCS, Kirchmair et al. previously clustered the DUD ligand sets by maximizing the dissimilarity of ECFP4 fingerprints. They then generated one, three, and five clusters per active set and selected the respective cluster centers as the query molecule for screening using ROCS. The comparison between these queries and our consensus clustering queries is presented in detail in the Supporting Information, in which best method for each DUD target is highlighted. Figure 11a shows the PARAFIT shape-based screening results for the 40 DUD targets using the PARAFIT-selected real center molecule and SHEF-selected queries, compared to using Kirchmair's center molecule as queries. It can be seen that using Kirchmair's center molecule as the query gives the best overall VS performance. However, for six of the targets, the PARAFIT center molecule query performs the best. For three targets, PARAFIT using the SHEF-selected molecule as query performs the best, and for five targets the PARAFIT center molecule gives very similar results to Kirchmair's center molecule. Figure 11b shows the corresponding results for the same queries in ROCS. Again, Kirchmair's center molecule is on the whole a better query than the PARAFIT center molecule and the SHEF-selected molecule. However for four targets, the PARAFIT center molecule performs better, and for eight targets the SHEF-selected molecule gives better results. Also for four targets, the PARAFIT center molecule gives very similar results to the Kirchmair center molecule. Figure 11c compares the shape-base VS performance using Kirchmair's center molecule in ROCS and the consensus pseudomolecule in PARAFIT. It can be seen that for sixteen of the targets, the PARAFIT consensus shape query gives the best performance and gives very similar results to Kirchmair's center molecule for four of the targets. Figure 11d compares the shape-base performance for the PARAFIT consensus pseudomolecule and Kirchmair's center molecule of one, three, and five clusters per active set. Screening with five Kirchmair compounds gives the best AUC values. However for three of the targets, using the consensus shape as the query improves the AUC, especially HIVRT, and for four of the targets the results are similar to Kirchmair AUC values.

**Consensus Clustering: Exploring Multiple Binding Sites.** According to the consensus clustering protocol (Figure 1), seven of the twelve “difficult” VS targets examined in Table 2 (i.e., CCR5, ALR2, P38, CDK2, PR, THROMBIN, and ACE) are predicted to be promiscuous.

**P38 Consensus Clustering.** The VS results presented above suggest that consensus shape-based clustering can help to identify targets that may have multiple binding sites. The ROC plots and AUC bar graphs previously analyzed show that the P38 and ALR2 targets could have multiple subsites. Hence, the P38 DUD ligand set was clustered using Ward's chemical fingerprints. Kelley's clustering method then found 15 clusters to be the optimal number. Hence, SH consensus shapes were calculated for each of the 15 groups. The consensus shapes of these clusters were compared in PARAFIT, and the resulting pairwise Tanimoto similarity scores were used in another round of Ward's hierarchical clustering to obtain three superconsensus (SC) clusters. Figure 12 shows the molecular superpositions and consensus shapes of the 15 groups used to calculate the final three SC shapes. These are referred to below as SC A, SC B, and SC C.

In order to explore how the members of the SC clusters might distribute themselves in the P38 pocket, the SC pseudomolecules were rigidly docked into the P38 pocket using Hex. This placed

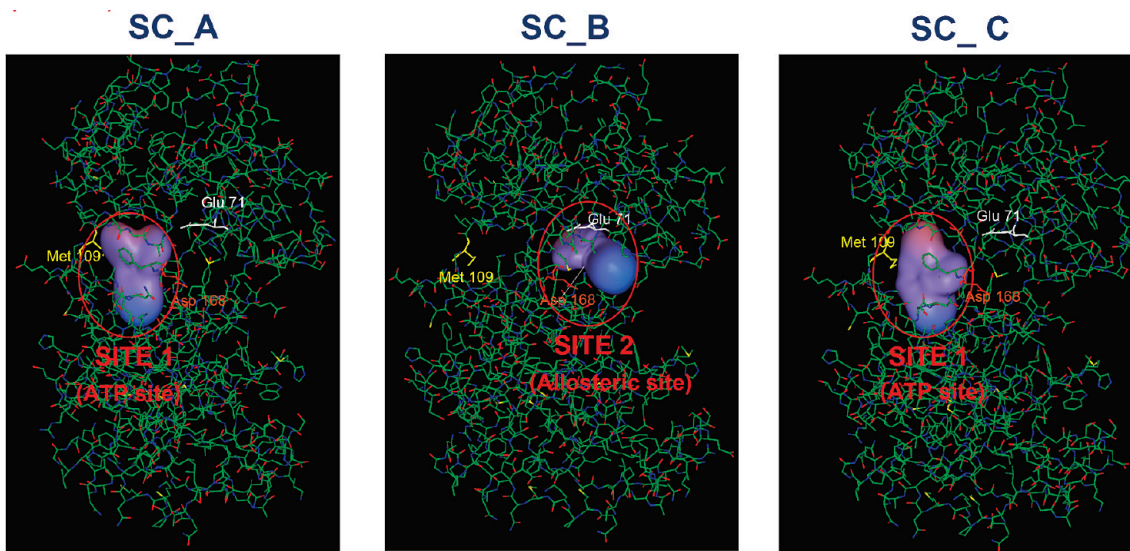


**Figure 13.** The P38 binding pocket subsites proposed by consensus VS and Hex blind docking. This figure shows close-up views of the docked SC pseudomolecules, annotated with the locations of known SDM binding site residues. In each case, the pseudomolecule was initially placed outside the P38 receptor pocket. SC A was blind docked onto one side of the P38 pocket. SC B was blind docked onto the opposite side of the pocket. SC C was blind docked in the same way as SC A. It can be seen that the consensus shape clustering results propose two binding subsites which agree with experimental information regarding the known ATP and allosteric subsites. The pyridinyl-imidazole inhibitors grouped in clusters C4 and C10 of SC A and other protein kinase inhibitors grouped in SC A and SC C are correctly docked into the ATP subsite, and diaryl urea inhibitors clustered in SC B are correctly docked into the allosteric subsite.

the SC A pseudomolecule on one side of the pocket, the SC B pseudomolecule on the opposite side, and SC C was placed in the same way as SC A. These docking poses are consistent with previous studies in which one group of molecules binds to an allosteric subsite next to the main pocket, making interactions with Glu 71 and Asp 168,<sup>16,42</sup> and another group binds to the ATP binding subsite, mainly making interactions with Met 109.<sup>43,44</sup> Figure 13 shows the rigid body docking poses obtained. It can be seen that the consensus shape clustering results propose two binding subsites which agree with experimental information regarding the known ATP and allosteric subsites. For example, the pyridinyl-imidazole inhibitors grouped in clusters C4 and C10 of SC A and other protein kinase inhibitors grouped in SC A and SC C are correctly docked into the ATP subsite,<sup>45</sup> and diaryl urea inhibitors clustered in SC B are correctly docked into the allosteric subsite.<sup>16</sup>

**ALR2 Consensus Clustering.** As described above, the DUD ligands for ALR2 were also initially clustered using chemical fingerprints. In this case, Kelley's method proposed five clusters as the optimal number. SH consensus shapes were then calculated for each of the five groups, and an all-against-all SH comparison of each consensus shape was calculated using PARAFIT. Another round of Ward's clustering then proposed three SC clusters. Figure 14 shows the molecular superpositions and consensus shapes of the five Ward's clusters used to calculate the final SH SC shapes and a dendrogram of the three main representative SC groups (also labeled A, B, and C). In this case, Hex docking placed SC A on one side of the pocket, binding to residues of the catalytic cleft (Tyr48, His110, and Trp111), whereas the larger SC B and C consensus molecules were docked into the whole pocket, i.e. binding to the catalytic cleft and to residues on the other side of the pocket (Thr113, Leu300, and Cys298).

There is considerable literature which indicates that ALR2 has broad substrate promiscuity.<sup>46–49</sup> To date, five five ligand scaffold

families have been characterized, represented by tolrestat, two members of the naphtho[1,2-d]isothiazole acetic acid series, sorbinil, and IDD 594.<sup>15</sup> The small and compact compounds (tolrestat, one naphtho[1,2-d]isothiazole acetic acid derivative, and sorbinil) bind to one side of the pocket, mainly the residues of the catalytic cleft (Tyr48, His110, and Trp111), whereas the larger compounds (such as IDD 594 and the other naphtho[1,2-d]isothiazole acetic acid derivative) also make similar interactions in the catalytic cleft. However, they occupy the whole pocket and bind to residues in the opposite side of the catalytic pocket (Leu 300, Thr113, Cys298, Ala 299, and Ser302).<sup>15</sup> Figure 15 shows the docking results obtained here. The agreement of consensus shape clustering with experimental information is clear. Consensus clustering finds a set of small compounds which are chemically similar to tolrestat in SC A and which bind near the catalytic cleft, while the other two SC clusters of compounds are chemically similar to IDD 594 and occupy the whole pocket (although with slightly different binding modes). This is consistent with the various crystal structures discussed above (i.e., ALR2 complexes have both large ligands which occupy the whole pocket and small ligands which bind to the catalytic cleft).

## ■ DISCUSSION

This study has investigated the importance of selecting a good query in shape-based VS and how consensus shape clustering can help to choose the right query. We have presented a new protocol using consensus shape clustering to understand difficult VS targets and to help identify promiscuous ligands and promiscuous targets.

Several previous studies have discussed how to optimize shape-based virtual screening. Kirchmair et al. found that using the center molecule of the compound set or using several different active compounds gave better VS performance than using a single crystallographic ligand as the query. For the 40

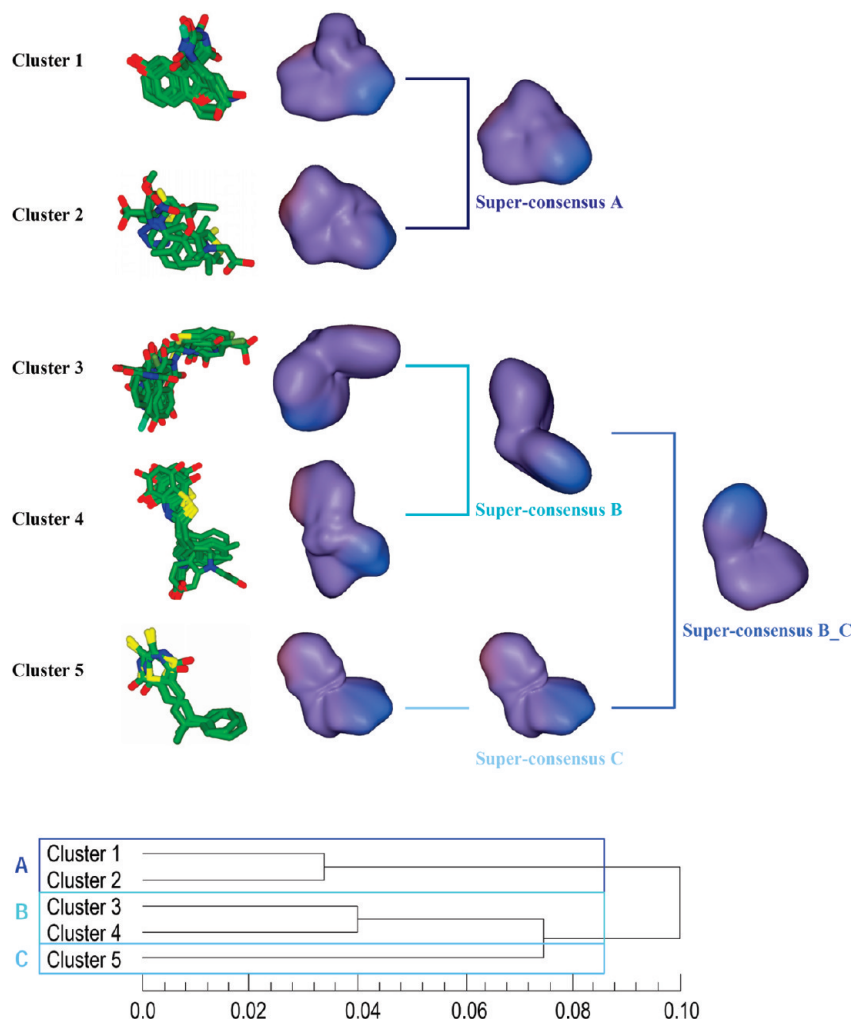


**Figure 14.** Molecular superpositions and consensus shapes of the five Ward's clusters used to calculate the final ALR2 SH SC shapes. The dendograms show the initial five ALR2 groups clustered using Ward's clustering of SH distances between the consensus surface shapes of each group. The three main SC groups, labeled A, B, and C, are highlighted.

DUD targets, Kirchmair's center molecules gave an average AUC 14% higher than the corresponding crystallographic ligand. Our SH-based consensus shapes builds on Kirchmair's approach by constructing more effective VS queries in the form of a small number of pseudomolecules. Hence it is not necessary to perform multiquery screening. Tawa et al.<sup>50</sup> explored the dependency of Kirchmair's screening results on the conformations of the center molecule. They showed that different conformations of the same molecule can yield very different VS results. Here, we broaden their approach by calculating shape-based clusters of the conformations of multiple actives in order to identify the best queries to be used.

Our study also shows that for some targets the crystallographic ligand does not always give the best VS performance. The X-ray ligand is not always as good a representation of the set of actives as the consensus pseudomolecule. Consensus clustering also gives an objective way to select a real center molecule which is often a useful representative example of a set of active ligands. As the results from this study show, the real center molecule also has very good VS performance, comparable to the consensus query.

With regard to the question of selecting the best query, conventional shape-based screening often assumes only a single

binding mode. Therefore, only those compounds in the database similar to the query will superpose correctly. However, some targets can have an active site which fits ligands in different ways. Hence, other potentially active compounds may be missed by conventional VS. This study has shown that the consensus clustering robustly captures and gives a fair way of combining the essential features of several known high-affinity ligands by encoding these in the form of a single representative pseudomolecule. This has been shown to be a good way of forming a query that can achieve high VS performance when dealing with difficult targets that have large ligand-binding pockets. We have proposed a new protocol based on consensus clustering to detect promising VS targets. This is useful when all ligands for a target cannot be superposed well. This protocol explores the possibility of accommodating them into different subsites, without requiring that they should all superpose well. We have applied this protocol to the 40 DUD targets, and we have analyzed in detail the P38 and ALR2 cases. As shown here for the P38 and ALR2 ligands, using consensus clusters improves VS enrichment, and this provides good evidence that these targets have multiple subsites. Docking the consensus pseudomolecules helps to identify pocket subsites which fit the consensus shapes. Hence,

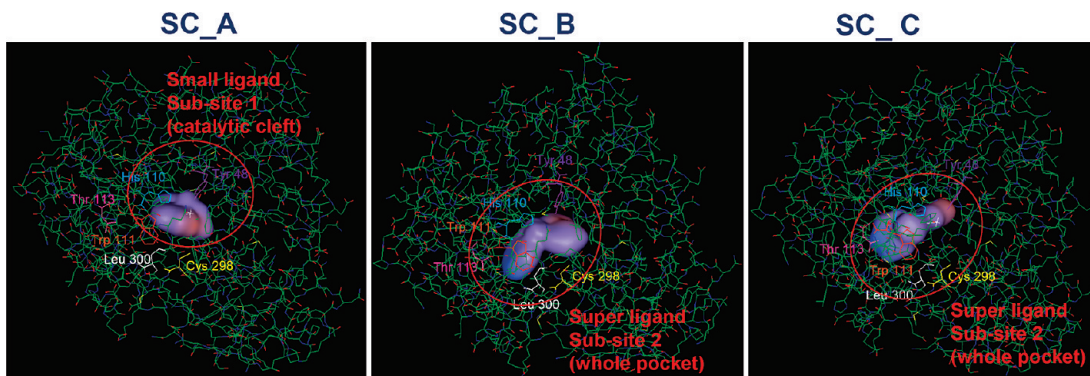


**Figure 15.** The ALR2 binding pocket subsites proposed by the consensus VS and Hex blind docking. This figure shows close-up views of the docked SC pseudomolecules, annotated with the locations of known SDM binding site residues. In each case, the pseudomolecule was initially placed outside the ALR2 receptor pocket. SC A was blind docked onto one side of the ALR2 pocket, whereas SC B and SC C pseudomolecules occupy the whole pocket. Consensus shape clustering and blind docking are able to find a set of compounds with small shape, binding to the catalytic cleft, while the other two SC clusters, comprising larger compounds, occupy the whole pocket (although with slightly different binding modes). These binding predictions are consistent with the known crystal structures.

the consensus pseudomolecule allows a cluster of compounds that bind to the same subsite to be represented.

Given the considerable number of DUD targets that seem capable of accommodating multiple ligands in a single pocket, we propose that promiscuous targets are more common than previously assumed and that future VS protocols should consider the possibility that a given target has multiple subsites. We propose that the protocol proposed here is a useful way to achieve this.

Finally, we have shown that shape clustering can help to identify promiscuous ligands. Cross-shape matching can be used as a first approach to identify promiscuous ligands and targets, saving a lot of computation time. The potential promiscuous targets in the DUD data set identified in this way are similar to the cross-docking results of Huang et al. but were calculated in just a few hours. Because ligand-based clustering is much faster than protein–ligand docking, this shows that using clustering techniques is a useful way to identify ligand promiscuity while avoiding the expense of all-against-all docking calculations.

## CONCLUSION

We have investigated the performance of different VS queries calculated in different ways for the 40 pharmaceutically relevant targets of the DUD database. The selection of the query compound(s) has been shown to be important for VS performance. We have shown that the crystallographic conformation is not always the best choice for good screening performance, especially when the receptor pocket can accommodate ligands in different ways. The SH consensus shape matching algorithm has been shown to be useful to construct a suitable query that can achieve high VS performance for these difficult targets. Furthermore, consensus clustering has been shown to be useful to detect promiscuous targets. Two examples have been explored in detail. Consensus clustering of the P38 ligands gives three SC pseudomolecules which we predict to dock to two subsites. Consensus clustering of the ALR2 ligands also gives three SC pseudomolecules for which subsequent docking proposes two subsites.

We have shown that if poor VS results are found, the possibility of multiple binding subsites can profitably be explored. Furthermore, clustering ligands which appear to bind into different subsites and performing VS as if each pocket is considered as a different target can be a useful way to improve VS

results. Finally, we have shown that shape-based clustering can help to identify promiscuous ligands. Cross-shape matching can be used as a fast way to identify cross-docking targets, saving a lot of computation time. Overall, we propose that promiscuous targets and promiscuous ligands are more common than previously assumed and that this possibility should be considered in practical VS protocols.

## ASSOCIATED CONTENT

**S Supporting Information.** Full details of the VS performance results for each DUD target and for each query used here are available as ROC plots and AUC bar charts. We also provide C-score bar charts for each of the 40 ligand set clusters and a table comparing the AUC values obtained using our queries with the results of Kirchmair et al. using their real center molecule. This material is available free of charge via the Internet at <http://pubs.acs.org>.

## AUTHOR INFORMATION

### Corresponding Author

\*Phone: +33-3-83593045. Fax: +33-3-83413079. E-mail: violeta.pereznueno@inria.fr

## ACKNOWLEDGMENT

The authors thank OpenEye Scientific Software Inc., ChemAxon, and Cepos Insilico Ltd. for providing Academic Licences for ROCS, JChem, and PARASURF, respectively. Part of this work is funded by the Agence Nationale de la Recherche, grant reference ANR-08-CEXC-017-01. V.I.P.N. is grateful for a Marie Curie IEF Fellowship.

## REFERENCES

- (1) Hawkins, P. C. D.; Skillman, A. G.; Nicholls, A. Comparison of shape matching and docking as virtual screening tools. *J. Med. Chem.* 2007, 50, 74–82.
- (2) Kirchmair, J.; Distinto, S.; Markt, P.; Schuster, D.; Spitzer, G. M.; Liedl, K. R.; Wolber, G. How To Optimize Shape-Based Virtual Screening: Choosing the Right Query and Including Chemical Information. *J. Chem. Inf. Model.* 2009, 49, 678–692.

- (3) Kellenberger, E.; Springael, J. Y.; Parmentier, M.; Hachet-Haas, M.; Galzi, J. L.; Rognan, D. Identification of nonpeptide CCR5 receptor agonists by structure-based virtual screening. *J. Med. Chem.* **2007**, *50*, 1294–303.
- (4) Wong, R. S. Y.; Bodart, V.; Metz, M.; Labrecque, J.; Bridger, G.; Fricker, S. P. Comparison of the Potential Multiple Binding Modes of Bicyclam, Monoclylam, and Noncyclam Small-Molecule CX<sub>C</sub> Chemokine Receptor 4 Inhibitors. *Mol. Pharmacol.* **2008**, *74*, 1485–1495.
- (5) Sato, H.; Shewchuk, L. M.; Tang, J. Prediction of Multiple Binding Modes of the CDK2 Inhibitors, Anilinopyrazoles, Using the Automated Docking Programs GOLD, FlexX, and LigandFit: An Evaluation of Performance. *J. Chem. Inf. Model.* **2006**, *46*, 2552–2562.
- (6) Williams, S.; Bledsoe, R. K.; Collins, J. L.; Boggs, S.; Lambert, M. H.; Miller, A. B.; Moore, J.; McKee, D. D.; Moore, L.; Nichols, J.; Parks, D.; Watson, M.; Wisely, B.; Willson, T. M. X-ray Crystal Structure of the Liver X Receptor  $\beta$  Ligand Binding Domain: Regulation by a Histidine-Tryptophan Switch. *J. Biol. Chem.* **2003**, *278*, 27138–27143.
- (7) Xu, Y.; Gurusiddappa, S.; Rich, R. L.; Owens, R. T.; Keene, D. N.; Mayne, R.; Höök, A.; Höök, M. *J. Biol. Chem.* **2000**, *275*, 38981–38989.
- (8) Rahimi, N. VEGFR-1 and VEGFR-2: two non-identical twins with a unique physiognomy. *Front Biosci.* **2006**, *11*, 818–829.
- (9) Taha, M. O.; Qandil, A. M.; Zaki, D. D.; Aldaben, M. A. Ligand-based assessment of factor Xa binding site flexibility via elaborate pharmacophore exploration and genetic algorithm-based QSAR modeling. *Eur. J. Med. Chem.* **2005**, *40*, 701–727.
- (10) Sok, D. E.; Kim, Y. B.; Choi, S. J.; Jung, C. H.; Cha, S. H. Multiple binding sites involved in the effect of choline esters on decarbamoylation of monomethylcarbamoyl- or dimethylcarbamoly-acetylcholinesterase. *Biochem. J.* **1994**, *301*, 713–720.
- (11) Zhao, Q.; Yang, G.; Mei, X.; Yuan, H.; Ning, J. Design of novel carbamate acetylcholinesterase inhibitors based on the multiple binding sites of acetylcholinesterase. *J. Pestic. Sci.* **2008**, *33*, 371–375.
- (12) Shelton, C. C.; Zhu, L.; Chau, D.; Yang, L.; Wang, R.; Djaballah, H.; Zheng, H.; Lia, Y.-M. Modulation of  $\gamma$ -secretase specificity using small molecule allosteric inhibitors. *Proc. Natl. Acad. Sci. U. S. A.* **2009**, *106*, 20228–20233.
- (13) Hammoudeh, D. I.; Follis, A. V.; Prochownik, E. V.; Metallo, S. J. Multiple Independent Binding Sites for Small-Molecule Inhibitors on the Oncoprotein c-Myc. *J. Am. Chem. Soc.* **2009**, *131*, 7390–7401.
- (14) Lee, Y. S.; Chen, Z.; Kador, P. F. Molecular Modeling Studies of the Binding Modes of Aldose Reductase Inhibitors at the Active Site of Human Aldose Reductase. *Bioorg. Med. Chem.* **1998**, *6*, 1811–1819.
- (15) Steuber, H.; Zentgraf, M.; La Motta, C.; Sartini, S.; Heine, A.; Klebe, G. Evidence for a Novel Binding Site Conformer of Aldose Reductase in Ligand-Bound State. *J. Mol. Biol.* **2007**, *369*, 186–197.
- (16) Pargellis, C.; Tong, L.; Churchill, L.; Cirillo, P. F.; Gilmore, T.; Graham, A. G.; Grob, P. M.; Hickey, E. R.; Moss, N.; Pavl, S.; Regan, J. Inhibition of p38 MAP kinase by utilizing a novel allosteric binding site. *Nat. Struct. Biol.* **2002**, *9*, 268–272.
- (17) Barrow, J. C.; Stauffer, S. R.; Rittle, K. E.; Ngo, P. L.; Yang, Z.; Selnick, H. G.; Graham, S. L.; Munshi, S.; McGaughey, G. B.; Holloway, M. K.; Simon, A. J.; Price, E. A.; Sankaranarayanan, S.; Colussi, D.; Tugusheva, K.; Lai, M.-T.; Espeseth, A. S.; Xu, M.; Huang, Q.; Wolfe, A.; Pietrak, B.; Zuck, P.; Levorse, D. A.; Hazuda, D.; Vacca, J. P. Discovery and X-ray Crystallographic Analysis of a Spiropiperidine Iminohydantoin Inhibitor of  $\beta$ -Secretase. *J. Med. Chem.* **2008**, *51*, 6259–6262.
- (18) Stachel, S. J.; Coburn, C. A.; Steele, T. G.; Crouthamel, M.-C.; Pietrak, B.-L.; Lai, M.-T.; Holloway, M. K.; Munshi, S. K.; Graham, S. L.; Vacca, J. P. Conformationally biased P3 amide replacements of  $\beta$ -secretase inhibitors. *Bioorg. Med. Chem. Lett.* **2006**, *16*, 641–644.
- (19) Pérez-Nueno, V. I.; Ritchie, D. W.; Borrell, J. I.; Teixidó, J. Clustering and classifying diverse HIV entry inhibitors using a novel consensus shape based virtual screening approach: Further evidence for multiple binding sites within the CCR5 extracellular pocket. *J. Chem. Inf. Model.* **2008**, *48*, 2146–2165.
- (20) Pérez-Nueno, V. I.; Ritchie, D. W.; Rabal, O.; Pascual, R.; Borrell, J. I.; Teixidó, J. Comparison of Ligand-Based and Receptor-Based Virtual Screening of HIV Entry Inhibitors for the CXCR4 and CCR5 Receptors Using 3D Ligand Shape-matching and Ligand-Receptor Docking. *J. Chem. Inf. Model.* **2008**, *48*, 509–533.
- (21) Huang, N.; Shoichet, B. K.; Irwin, J. J. Benchmarking sets for molecular docking. *J. Med. Chem.* **2006**, *49*, 6789–6801.
- (22) Lin, J.; Clark, T. An Analytical, Variable Resolution, Complete Description of Static Molecules and Their Intermolecular Binding Properties. *J. Chem. Inf. Model.* **2005**, *45*, 1010–1016.
- (23) Ritchie, D. W.; Kemp, G. J. L. Protein Docking Using Spherical Polar Fourier Correlations. *Proteins: Struct., Funct., Genet.* **2000**, *39*, 178–194.
- (24) Mavridis, L.; Hudson, B. D.; Ritchie, D. W. Toward High Throughput 3D Virtual Screening Using Spherical Harmonic Surface Representations. *J. Chem. Inf. Model.* **2007**, *47*, 1787–1796.
- (25) Venkatraman, V.; Pérez-Nueno, V. I.; Mavridis, L.; Ritchie, D. W. Comprehensive Comparison of Ligand-Based Virtual Screening Tools Against the DUD Dataset Reveals Limitations of Current 3D Methods. *J. Chem. Inf. Model.* **2010**, *50*, 2079–2093.
- (26) Giganti, D.; Guillemain, H.; Spadoni, J.-L.; Nilges, M.; Zagury, J.-F.; Montes, M. Comparative Evaluation of 3D Virtual Ligand Screening Methods: Impact of the Molecular Alignment on Enrichment. *J. Chem. Inf. Model.* **2010**, *50*, 992–1004.
- (27) OpenEye Scientific Software Inc.: Santa Fe, NM, 1997–2009.
- (28) Beautrait, A.; Leroux, V.; Chavent, M.; Ghemtio, L.; Devignes, M.-D.; Smail-Tabbone, M.; Cai, W.; Shao, W.; Moreau, G.; Bladon, P.; Yao, Maigret, B. J. Multiple-step virtual screening using VSM-G: overview and validation of fast geometrical matching enrichment. *J. Mol. Model.* **2008**, *14*, 135–148.
- (29) Cai, W.; Xu, J.; Shao, X.; Leroux, V.; Beautrait, A.; Maigret, B. SHEF: a vHTS geometrical filter using coefficients of spherical harmonic molecular surfaces. *J. Mol. Model.* **2008**, *14*, 393–401.
- (30) The Cambridge Crystallographic Data Centre, Cambridge, UK, 2004–2009.
- (31) CEPOS InSilico Ltd.: Erlangen, Germany, 2009. <http://www.ceposinsilico.de/> (accessed June 24, 2009).
- (32) Molecular Operating Environment (MOE), Chemical Computing Group Inc, Montreal, QC (Canada), 2008.10 Release, 2009.
- (33) Kirchmair, J.; Markt, P.; Distinto, S.; Wolber, G.; Langer, T. Evaluation of the performance of 3D virtual screening protocols: RMSD comparisons, enrichment assessments, and decoy selection. What can we learn from earlier mistakes? *J. Comput.-Aided Mol. Des.* **2008**, *22*, 213–228.
- (34) OMEGA, OpenEye Scientific Software Inc., Santa Fe, NM, USA, v. 2.3.2, 2010.
- (35) Triballeau, N.; Acher, F.; Brabet, I.; Pin, J.-P.; Bertrand, H.-O. Virtual Screening Workflow Development Guided by the “Receiver Operating Characteristic” Curve Approach. Application to High-Throughput Docking on Metabotropic Glutamate Receptor Subtype 4. *J. Med. Chem.* **2005**, *48*, 2534–2547.
- (36) Mackey, M. D.; Melville, J. L. Better than Random? The Chemotype Enrichment Problem. *J. Chem. Inf. Model.* **2009**, *49*, 1154–1162.
- (37) Von Korff, M.; Freyss, J.; Sander, T. Comparison of Ligand- and Structure-Based Virtual Screening on the DUD Data Set. *J. Chem. Inf. Model.* **2009**, *49*, 209–231.
- (38) Truchon, J.; Bayly, C. I. Evaluating Virtual Screening Methods: Good and Bad Metrics for the “Early Recognition” Problem. *J. Chem. Inf. Model.* **2007**, *47*, 488–508.
- (39) Ward, J. H. Hierarchical Grouping to Optimize an Objective Function. *J. Am. Statist. Assoc.* **1963**, *58*, 236–244.
- (40) JKlustor, v5.3.4; a module of JChem. ChemAxon Ltd.: Budapest, Hungary, 2010. <http://www.chemaxon.com/jchem/doc/user/JKlustor.html> (accessed June 28, 2010).
- (41) Kelley, L. A.; Gardner, S. P.; Sutcliffe, M. J. An automated approach for clustering an ensemble of NMR-derived protein structures into conformationally-related subfamilies. *Protein Eng.* **1996**, *9*, 1063–1065.
- (42) Cirillo, P. F.; Gilmore, T. A.; Hickey, E.; Regan, J.; Zhang, L. H. Aromatic Heterocyclic Compounds as Antiinflammatory Agents. World Patent Application WO-00043384, 2000.

- (43) Lee, J. C.; Badger, A. M.; Griswold, D. E.; Dunnington, D.; Truneh, A.; Votta, B.; White, J. R.; Young, P. R.; Bender, P. E. Bicyclic imidazoles as a novel class of cytokine biosynthesis inhibitors. *Ann. N.Y. Acad. Sci.* **1993**, *696*, 149–70.
- (44) Tong, L.; Pav, S.; White, D. M.; Rogers, S.; Crane, K. M.; Cywin, C. L.; Brown, M. L.; Pargellis, C. A. A highly specific inhibitor of human p38 MAP kinase binds in the ATP pocket. *Nat. Struct. Biol.* **1997**, *4*, 311–316.
- (45) Lee, J. C.; Laydon, J. T.; McDonnell, P. C.; Gallagher, T. F.; Kumar, S.; Green, D.; McNulty, D.; Blumenthal, M. J.; Heys, J. R.; Landvatter, S. W.; Strickler, J. E.; McLaughlin, M. M.; Siemens, I. R.; Fisher, M.; Livi, G. P.; White, J. R.; Adams, J. L.; Young, P. R. A protein kinase involved in the regulation of inflammatory cytokine biosynthesis. *Nature* **1994**, *372*, 739–746.
- (46) Da Settimo, F.; Primofiore, G.; La Motta, C.; Sartini, S.; Taliani, S.; Simorini, F.; Marini, A. M.; Lavecchia, A.; Novellino, E.; Boldrini, E. Naphtho [1,2-d] isothiazole acetic acid derivatives as a novel class of selective aldose reductase inhibitors. *J. Med. Chem.* **2005**, *48*, 6897–6907.
- (47) Urzhumtsev, A.; Tete-Favier, F.; Mitschler, A.; Barbanton, J.; Barth, P.; Urzhumtseva, L.; Biellmann, J.-F.; Podjarny, A. D.; Moras, D. A specificity” pocket inferred from the crystal structures of the complexes of aldose reductase with the pharmaceutically important inhibitors tolrestat and sorbinil. *Structure* **1997**, *5*, 601–612.
- (48) Steuber, H.; Zentgraf, M.; Podjarny, A. D.; Heine, A.; Klebe, G. High resolution crystal structure of aldose reductase complexed with the novel sulfonyl-pyridazinone inhibitor exhibiting an alternative active site anchoring group. *J. Mol. Biol.* **2006**, *356*, 45–56.
- (49) El-Kabbani, O.; Wilson, D. K.; Petrash, J. M.; Quiocho, F. A. Structural features of the aldose reductase and aldehyde reductase inhibitor binding sites. *Mol. Vision* **1998**, *4*, 19–25.
- (50) Tawa, G. J.; Baber, J. C.; Humblet, C. Computation of 3D queries for ROCS based virtual screens. *J. Comput.-Aided Mol. Des.* **2009**, *23*, 853–868.
- (51) Pérez-Nueno, V. I.; Venkatraman, V.; Mavridis, L.; Clark, T.; Ritchie, D. W. Using spherical harmonic surface property representations for ligand-based virtual screening. *Mol. Inf.* **2011**, *30*, 151–159.